Nanoscale

PAPER

View Article Online
View Journal | View Issue

Cite this: *Nanoscale*, 2025, **17**, 2078

Hydroxyapatite nanoparticle mediated delivery of full length dystrophin gene as a potential therapeutic for the treatment of Duchenne muscular dystrophy†

Pooja Kotharkar,[a] Indrani Talukdar, *[a] Sutapa Roy Ramanan, [b] Keerthi Ramesh,[c] Arun Shastry[c] and Meenal Kowshik *[a]

Received 23rd September 2024,
Accepted 2nd December 2024

DOI: 10.1039/d4nr03906h

rsc.li/nanoscale

Duchenne muscular dystrophy (DMD) is a severe genetic disorder characterized by progressive muscle degeneration, primarily affecting young males. In this study, we investigated arginine-modified hydroxyapatite nanoparticles (R-HAp) as a novel non-viral vector for DMD gene therapy, particularly for delivering the large 18.8 kb dystrophin gene. Addressing the limitations of traditional adeno-associated viral vectors, R-HAp demonstrated efficient binding and delivery of the dystrophin plasmid to DMD patient-derived skeletal muscle cells. Using confocal imaging and RT-PCR analysis, our results showed effective gene delivery and expression in both mouse myotubes and patient-derived cells, with sustained expression evident up to 5 days post transfection. The patient-derived myotubes also showed dystrophin protein production 7 days post transfection. These findings suggest R-HAp nanoparticles as a promising and cost-effective alternative for DMD treatment, highlighting their potential for overcoming current gene therapy challenges.

1 Introduction

Duchenne muscular dystrophy (DMD) is an X-linked, degenerative muscular disease caused by mutations in the dystrophin gene which is one of the largest protein-coding genes (2.5 Mb) in the human genome. It affects 1 in 5000 males worldwide. The dystrophin gene has 79 exons generating a 427 kDa protein with 3685 amino acids and is located at position Xp21.1 of the X chromosome.[1] Dystrophin is widely expressed in skeletal, cardiac and smooth muscles, and a small amount at specific locations in the CNS.[2]

Approximately 60% of mutations in patients with DMD are deletions and 11% are duplications, with the remainder being small mutations affecting the coding sequence and splice sites.[3] Deletions and duplications occur predominantly in two hotspots of the DMD gene, located at exons 3–9 and 45–55.[4] Clinically, the DMD phenotype includes reduced motor functions, Gowers' sign, increased creatine kinase, scoliosis, and toe walking.[5] Characterized by progressive muscle degeneration, individuals with DMD become wheelchair bound during their teenage years and face severe respiratory and cardiac complications, often leading to death. Currently, there is no effective treatment to prevent or restore the muscle deterioration in DMD patients.

The emerging field of gene therapy offers a beacon of hope in this challenging landscape. Recent advances have centered on restoring dystrophin expression, a strategy with the potential to alter the course of the disease fundamentally. However, conventional methods, such as the use of Adeno-Associated Virus (AAV) vectors, come with limitations, as the dystrophin gene is ~11.5 kb long which is beyond the packaging capacity of the viral vectors.[6,7] Often referred to as a 'million-dollar therapy', the high cost of AAV based gene therapy is primarily attributed to high manufacturing cost and challenges associated with scaling up. Difficulties with the purification of recombinant-AAV particles from cellular and viral impurities and inherent batch-to-batch variation of vector potency all impact production costs. Moreover, immune response by natural antibodies found extensively in the human population owing to natural AAV infection can effectively block AAV gene delivery. This underscores the urgent need for innovative, cost-effective alternatives in gene therapy approaches.[8–10]

[a]*Biological Sciences Department, Birla Institute of Technology and Science Pilani, K K Birla Goa Campus, Goa, India. E-mail: meenal@goa.bits-pilani.ac.in, indranit@goa.bits-pilani.ac.in*
[b]*Chemical Engineering Department, Birla Institute of Technology and Science Pilani, K K Birla Goa Campus, Goa, India*
[c]*Dystrophy Annihilation Research Trust, Bangalore, India*
† Electronic supplementary information (ESI) available. See DOI: https://doi.org/10.1039/d4nr03906h

While gene therapy has advanced, existing methods often involve compromises. For instance, strategies like the use of mini- or micro-dystrophin aim to produce a shorter dystrophin protein, somewhat alleviating symptoms akin to Becker muscular dystrophy.[8,9] Similar approaches like exon skipping, gene editing using CRISPR/Cas9, and myoblast transplantation, though promising, are yet to be used as a definitive cure and are still out of reach. This gap highlights the necessity for more advanced therapies that can effectively deliver the full-length dystrophin gene, directly addressing the disease at its genetic foundation.[8–11]

Hydroxyapatite nanoparticles (HAp NPs) have emerged as a viable solution to the intricate challenges of gene delivery in Duchenne Muscular Dystrophy (DMD). Their biocompatibility is coupled with a unique capacity for nucleic acid binding, crucial for delivering the sizable dystrophin gene. The strategic modification of HAp NPs with arginine enhances their gene transfer efficiency, potentially addressing the limitations of existing delivery systems in DMD therapy.[11]

In this work, we have used arginine-conjugated hydroxyapatite nanoparticles (R-HAp) to deliver an 18.8 kb dystrophin plasmid. We quantified the stability and affinity of the R-HAp and dystrophin plasmid complex to analyze their binding interaction. Additionally, we analyzed transfection assays in mouse myotubes to assess the internalization efficiency of the R-Hap–plasmid complex. This approach was also extended to evaluate gene expression in skeletal muscle cells derived from DMD patient skin fibroblasts, providing insights into the utility of R-HAp Nps for dystrophin gene therapy.

2 Materials and methods

The chemicals and reagents used were of analytical grade. For nanoparticle synthesis, $CaCl_2{\cdot}2H_2O$ was purchased from Hi-media, India. Dimethyl sulfoxide (DMSO), orthophosphoric acid (H_3PO_4), acetylacetone, ammonia, and the anti-mouse secondary antibody were purchased from Merck, India. Arginine was purchased from Sigma Aldrich India. The undifferentiated C2C12 cell line (mouse myoblast cells) was purchased from NCCS, Pune, India. Dulbecco's modified Eagle's medium high glucose (DMEM), fetal bovine serum (FBS), and Dulbecco's phosphate buffered saline (PBS), trypsin-EDTA solution, MTT (3-(4,5-dimethylthiazol-2-yl)-2,5-diphenyltetrazolium bromide), antibiotic and antimycotic solutions, RNA Xpress reagent, horse serum and Proteinase K were obtained from Hi-Media, India. Ham's F-10 Nutrient mix fetal bovine serum and horse serum for human skeletal muscle cell culture were purchased from Gibco, USA. A high-capacity cDNA kit, Lipofectamine 3000, dystrophin recombinant rabbit monoclonal antibody, and polyclonal anti-rabbit secondary antibody were supplied by Invitrogen, U.S.A. Beta actin monoclonal antibody was purchased from Proteintech, USA. Q-PCR Master mix (SYBR) was obtained from SMOBIO. Hotstart was purchased from Takara Bio, India. The plasmid p37-2iDMD-LR was a gift from Michele Calos (Addgene plasmid # 88892; **https://n2t.net/addgene:88892**; RRID: Addgene_88892).[12] Clarity Western ECL blotting substrate was purchased from BIO-RAD, India.

2.1 Synthesis

The synthesis of arginine modified HAp (R-HAp) was carried out at room temperature. Briefly, 2 M $CaCl_2{\cdot}2H_2O$ was dissolved in 2.5 mL of DMSO under continuous stirring at 50 rpm followed by dropwise addition of 1 M H_3PO_4, and the final volume was made up to 5 mL using acetylacetone. After stirring the reaction solution for 30 min, the pH was adjusted to 10 using liquid NH_3, and stirring continued for 30 min. Finally, arginine (0.4% w/v) was dissolved in deionized water and added to the sol dropwise and stirred for 30 min. The mixture was dialyzed for 24 h against deionized water and dried at room temperature. The obtained powder was used as such, or ultrasonic processing of the suspension was carried out to ensure adequate dispersion wherever applicable.

2.2 Dystrophin plasmid

The ***p37-2iDMD-LR*** plasmid (henceforth referred to as dystrophin plasmid) is a full-length DMD luc-red plasmid with a size of 18.8 kb, which co-expresses human dystrophin, firefly luciferase and mCherry in mammalian cells. The plasmid was transformed into *E. coli* DH5α. The harvested bacterial culture was lysed and collected by centrifugation after which it was applied to a silica column for binding of DNA in the presence of a high salt concentration. The adsorbed DNA was washed to remove contaminants, and the pure plasmid DNA was eluted in the elution buffer. The concentration of the purified plasmid was determined spectrophotometrically.

2.3 Characterization

Preliminary characterization of the synthesized R-HAp was carried out by X-ray diffraction measurements using a Rigaku Mini-Flex II powder X-ray diffractometer with a scan range of 2θ = 20–60° employing Cu Kα (1.54 Å) radiation. The Debye–Scherrer formula was used to determine the crystal size:

$$D = \frac{k\lambda}{\beta \cos\theta}$$

where λ is the wavelength of the X-ray, k is a constant with a value of 0.94, β is the full width (radians) at half-maximum of the signal, and θ is the Bragg angle. The FT-IR spectrum was recorded from 4000 to 400 cm^{-1} using the IR affinity-1S Fourier transform infrared spectrophotometer (Shimadzu). TEM and high-resolution TEM (HR-TEM) along with selected-area electron diffraction (SAED) measurements were performed using FEI Tecnai G2, F30 with a field-emission gun operating at 300 kV. Surface charge analysis with ζ potential was performed using a zeta-potential analyzer (Delsa Nano S, Beckman Coulter, U.S.A.) at pH 7.

2.4 Binding efficiency

The ability of R-HAp to form a complex with the plasmid was studied by keeping the amount of plasmid constant (50 ng) and varying the amount of R-HAp. The complex was incubated

at room temperature for 20 minutes and loaded on an agarose gel (0.7%, ethidium bromide included for visualization) for 60 minutes at 80 V cm^{-1}. Unbound plasmid was used as a positive control. The images were obtained using a UV transilluminator and band intensities were quantified using the Geldoc 2000 gel documentation system.

2.5 Cell culture

(a) Mouse myoblast cell culture. Mouse myoblast C2C12 cells were purchased from NCCS, Pune, and maintained in Dulbecco's modified Eagle's medium (DMEM), supplemented with 10% v/v fetal bovine serum (FBS) and 1% v/v penicillin and streptomycin antibiotic solution (cell culture media). Cells were incubated at 37 °C with 5% CO_2 in air and sub-cultured on alternate days.

For differentiation, C2C12 cells were seeded at a density of 5×10^4 cells per well in a 6-well tissue culture treated plate and allowed to grow for 24 hours in the presence of cell culture media. After that, the media were changed using differentiation media consisting of DMEM, supplemented with 2% v/v horse serum and 1% v/v penicillin and streptomycin antibiotic solution [differentiation media]. Media change was carried out every 24 hours and the cells were subjected to experiments after 7 days once the differentiated cell morphology was obtained.

(b) Patient derived myoblast cell culture. Experiments related to DMD patient cells were carried out at the Dystrophin Annihilation Research Trust (DART), Bangalore. Ethical clearance was obtained by DART, Bangalore, to carry out the *in vitro* experiments using skin fibroblast cells obtained by skin biopsy of a DMD positive patient. The patient exhibited a hemizygous variation in exon 44 of the DMD gene (X chromosome) resulting in the formation of a stop codon at 2098 and a premature truncation of the protein.[13] Patient skin fibroblasts were converted to myoblast cells *in vitro* using the MyoD expressing the adeno viral vector.[14] In short, skin fibroblasts were allowed to grow up to 80% confluence prior to the transformation process. Subsequently, the washed and pelleted cells were suspended in differentiation media (DMEM along with 2% v/v horse serum and 1% v/v penicillin and streptomycin antibiotic solution). The transfection agent, Ad5.f50.AdApt.MyoD, was added to the cell suspension and seeded on the poly D-lysine and Matrigel treated tissue culture plates for further experimentation. Complete media change was carried out with differentiation medium after 24 hours of transfection and continued for 96 hours of transfection for the completion of myogenesis.

(c) Human skeletal muscle cell culture. Skeletal muscle cells were received from DART, Bangalore. The cells were maintained in F-10 nutrient mixture (Ham), supplemented with 20% v/v fetal bovine serum (FBS) and 1% v/v penicillin and streptomycin antibiotic solution (cell culture media). Cells were incubated at 37 °C with 5% CO_2 in air and subcultured on alternate days.

For differentiation, skeletal muscle cells were seeded at a density of 5×10^4 cells per well in a 6-well tissue culture treated plate and allowed to grow for 24 hours in the presence of cell culture media. After that, a media change was given with differentiation media consisting of F-10 nutrient mixture, supplemented with 2% v/v horse serum and 1% v/v penicillin and streptomycin antibiotic solution [differentiation media]. Media change was carried out every 24 hours and the cells were subjected to experiments after 7 days once the differentiated cell morphology was obtained.

2.6 MTT assay for cytotoxicity analysis

For this experiment, 5×10^4 cells were seeded in 96-well plates and allowed to grow for 24 hours. R-HAp sol ranging in concentration from 50 to 500 μg ml^{-1} was added to the wells and the complex was allowed to incubate with the cells for 24 or 48 hours. Subsequently, cells were given a PBS wash and a solution of 0.5 mg ml^{-1} of MTT reagent in DMEM was added to each well of the plate. The plate was kept in the dark at 37 °C for 4 hours, the absorbance was measured using a spectrophotometer at 540 nm and the cell survival percentage was calculated. Three experimental replicates were taken for calculation of the cell viability percentage.

2.7 Internalization of the dystrophin plasmid : R-HAp complex

For studying the internalization of R-HAp, C2C12 cells were seeded onto sterile coverslips on a 12-well plate and allowed to attach. In parallel, the required amount of R-HAp was suspended in DMEM to prepare a working stock. The resulting suspension was sonicated using a probe sonicator. R-HAP suspension equivalent to 400 μg of R-HAp by weight was incubated at room temperature for 20 minutes with 50 ng of the dystrophin plasmid to allow the complex to form. Subsequently, the plasmid : R-HAp complex was added to the cells in a serum free, antibiotic free media and incubated for 6 hours. A media change was given and the cells were replenished with fresh media containing 10% serum and antibiotics. After 48 hours post-addition of the nano-complex, the cells on the coverslip were fixed using 4% v/v formaldehyde solution in PBS. Cells transfected using the commercially available transfection reagent Lipofectamine 3000, using the manufacturer's protocol, served as a positive control, while the untreated cells were considered as the negative control. The imaging was performed using confocal microscopy (Olympus Corporation FV3000).

R-HAp mediated transfection of the dystrophin plasmid was also carried out on normal human skeletal muscle cells and DMD positive patient cells. The methodology was similar to that used for mouse C2C12 cells. The slides were observed for mCherry gene expression after 48 hours for red fluorescence using a confocal microscope.

Transfection efficiency was calculated as per the following formula:

$$\text{Transfection efficiency} = (\text{no. of transfected cells})/(\text{total no. of cells})$$

Here the cells showing mCherry gene expression were taken as the transfected cells.

2.8 Evaluation of gene expression by RT-PCR

RNA was extracted using Trizol reagent 24 and 48 h post transfection from the undifferentiated C2C12 cells and 1–5 days post transfection from the differentiated C2C12 cells. RNA was also extracted from R-HAp transfected DMD patient cells and was further used for analysis of the dystrophin gene. Total RNA was quantified with a spectrophotometer (Nanodrop LITE, Thermo Scientific), and 1 μg of RNA was used to generate cDNA according to the manufacturer's protocol (Invitrogen, U. S.A.). For amplification of mCherry, dystrophin and GAPDH genes, specific primers were used (Table 1) and the thermal profile was obtained using standard amplification protocols. Amplification was confirmed by agarose gel electrophoresis.

2.9 Evaluation of gene expression by q-PCR

RNA was extracted from control and transfected C2C12 cells after 24 hours and 48 hours of R-HAp mediated transfection as discussed before. For q-PCR analysis, the mCherry gene was taken as a target gene and 18S was used as a housekeeping gene. q-PCRs were carried out on an AriaMx real-time PCR System (Agilent) with SYBR Green q-PCR Master Mix (SMOBIO). The annealing temperatures for both the genes were kept at 52 °C and amplification was carried out for 40 cycles. The Cq (ΔR) values of the transfected samples were normalized using Cq (ΔR) values of 18 S housekeeping genes.

Target gene	Gene primer	Product size
18-s	F: 5′ CATGGCCGTTCTTAGTTGGT-3′ R: 5′CGCTGAGCCAGTCAGTGTAG-3′	250 bp

The primer used for mCherry was the same as that for the RT-PCR gene shown above.

2.10 Western blot analysis

For protein analysis by western blot, DMD patient cells were seeded at a density of 5×10^4 cells per well in 6-well plates. The cells were allowed to differentiate for a period of 7 days in differentiating media and transfected with the DMD plasmid using R-HAp Nps as described previously. Protein was extracted post 7 days of transfection and used for western blot analysis. For protein extraction, the cells were trypsinized, washed twice with sterile PBS buffer and subjected to lysis using RIPA buffer (HiMedia) containing protease-inhibitor cocktail (HiMedia). Cell lysates were kept on ice for 30 min with intermediate agitation and then subjected to centrifugation at 4 °C for 15 min at 12 000 rpm. The total cellular proteins were collected, and protein concentrations were quantified by Bradford assay using a commercial protein standard (1 mg ml^{-1}) (Himedia). Protein extracted from un-transfected patient cells served as the negative control and protein extracted from normal human skeletal muscle cells served as the positive control. The total cellular proteins (30 μg) were separated by SDS polyacrylamide gel electrophoresis and the transfer was carried out using a PVDF membrane at 25 V by the wet transfer method for 15 hours. The membrane was blocked using 5% fat milk. The antibodies used were of the following specifications: monoclonal rabbit primary antibody anti-Dystrophin 1 : 1000 (Invitrogen) and monoclonal mouse primary antibody anti-β-actin, 1 : 20 000 (Proteintech). The membranes were washed and incubated for 1 hour with a corresponding horseradish peroxidase-conjugated secondary antibody as follows: polyclonal anti-rabbit secondary antibody, 1 : 3000 (Invitrogen) and polyclonal anti-mouse secondary antibody, 1 : 5000 (Merck). The specific proteins were visualized on X-ray films using an enhanced chemiluminescence detection system (BIO-RAD).

Table 1 Primer sequences for RT-PCR Amplification of target genes

Target gene	Gene primer	Product size
mCherry	F: 5′CAGGACGGCGAGTTCATCTA-3′ R: 5′GTCTTGACCTCAGCGTCGTA-3′	197 bp
Dystrophin	F 5′CAGCGGCAAACTGTTGTCAG-3′ R-5′GCTGCTCTTTTCCAGGTTCAAG-3′	274 bp
GAPDH	F: 5′-GATGCCCCCATGTTTGTGAT-3′ R: 5′-GGTCATGAGCCCTTCCACAAT-3′	150 bp

2.11 Statistical analysis

Statistical analysis was carried out using either one-way ANOVA (followed by Tukey's test if required) or Student's *t*-test ($*p < 0.05$, $**p < 0.005$, and $***p < 0.001$) for the experiments as required. All the experiments were performed in replicates and controls with respect to the experiments were maintained.

3 Results

3.1 Characterization of the synthesized nanoparticles

The main objective of the gene delivery vehicle is to efficiently bind the cargo and deliver it successfully to the target site. With this aim, HAp Nps were functionalized with various moieties to facilitate robust binding with the plasmid. The two key moieties which aided nucleic acid binding were octa arginine (R8 HAp) and arginine (R-HAp). During the binding studies (which will be discussed further) it was evident that in comparison with R8 HAp, the R-HAp Nps displayed efficient binding and at a lower concentration as compared to R8 HAp. Hence, this section will describe in detail the characterization of R-HAp Nps.

Arginine functionalized R-HAp Nps were synthesized by a modified sol–gel method and dried to obtain a pale white colored powder. The synthesized nanoparticles were analyzed using physical characterization techniques like FTIR spectroscopy, XRD, HR-TEM and zeta potential analysis. The FTIR spectra for 0.4% R-HAp is shown in Fig. 1A. The band in the region around 3500 cm^{-1} corresponds to –OH stretching vibrations and that at 1422 cm^{-1} corresponds to the stretching mode of CO_3^{2-} groups.

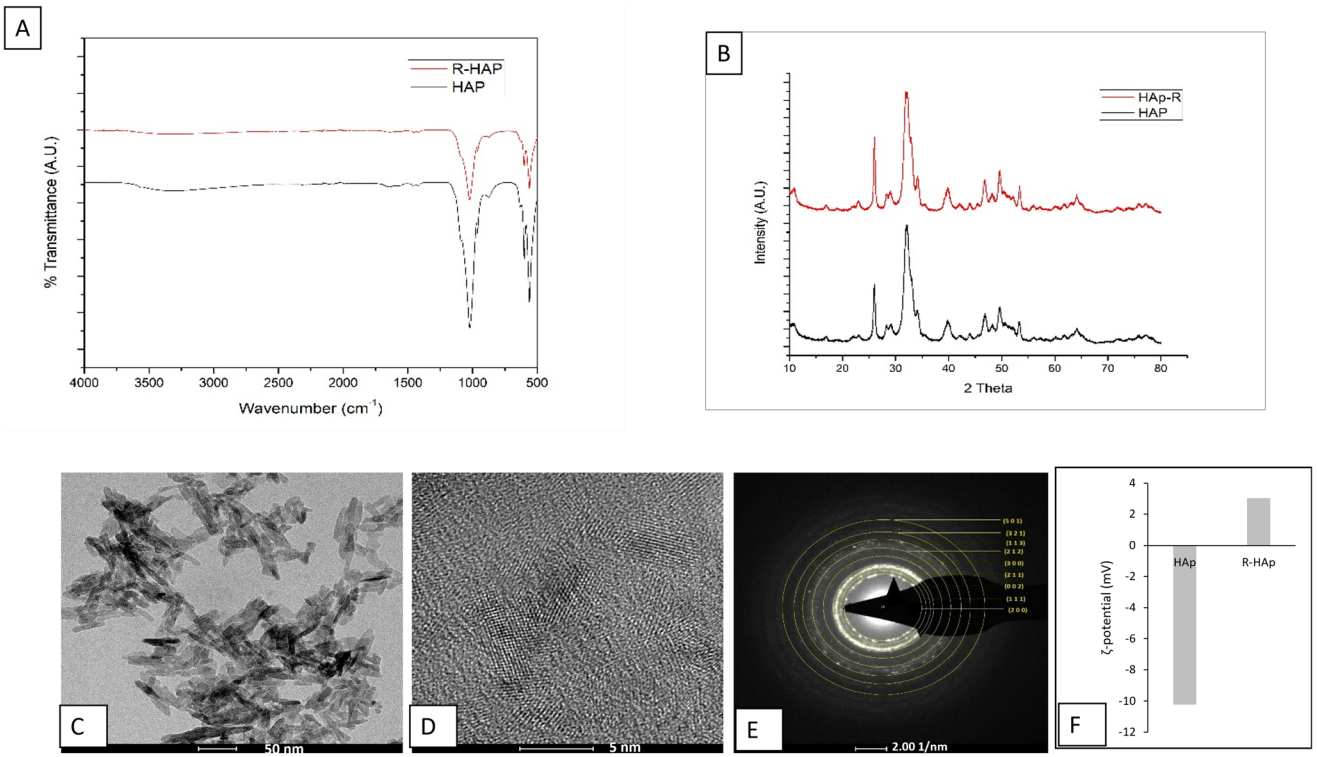

Fig. 1 Characterization of R-HAp nanoparticles. (A) FTIR spectrum of R-HAp and HAp Np. (B) XRD spectrum of R-HAp and HAp Np. (C) TEM and (D) HR-TEM micrographs and (E) SAED pattern. (F) ζ-Potential measurements of R-HAp Nps, compared with un-functionalized HAp NPs.

The bands of NH_2 and amide I associated with arginine were observed at ~1448 and ~1644 cm.$^{-1}$ The strongest band between 1000 and 1100 cm^{-1} is associated with the P–O stretching vibration of the phosphate group. The double band between 559 and 602 cm^{-1} is attributed to the bending mode of the P–O bond in the phosphate group.[15] The absorption observed at 1644 cm^{-1} is due to the symmetric stretching mode of NH_3 which overlaps with the vibration of H_2O at 1630 cm^{-1}, leading to the broadening of the absorption band. The symmetric stretching of NH_3 group is observed at 1454 cm^{-1} confirming the functionalization of HAp Nps with arginine.[15–17]

The XRD spectra of the as-synthesized R-HAp exhibited representative peaks for HAp hexagonal crystals corresponding to ICDD card no. 09-0432. Characteristic peaks at 25.55°, 32.51°, and 34.91° corresponding to *hkl* lattices of (002), (211), and (300) were observed (Fig. 1B), indicating that inclusion of arginine did not affect the HAp crystal structure. The crystallite size for the (211) peak and full-width half-maxima (FWHM) calculated using the Debye–Scherrer formula were 5.15 nm and 1.69 nm, respectively.[16]

The HR-TEM micrographs show a thin rod-shaped morphology with slightly rounded edges. R-HAp Nps had an average length of 33.04 ± 8.86 nm and a width of 6.64 ± 1.81 nm. Uniform lattice fringes were observed, which indicate the crystalline nature of R-HAp Nps (Fig. 1D). The polycrystalline nature of the HAp phase can be confirmed using the SAED ring pattern. The SAED patterns of R-HAp showed hexagonal crystalline planes of (200), (111), (002), (211), (300), (212), (113), (321), (501) in sequence (Fig. 1E).

The ζ-potential (Fig. 1F) value of R-HAp was found to be 3.04 while originally for the un-functionalized HAp Nps, it was −10.22 mV. This shows that the functionalization of HAp Nps with arginine gives an overall positive charge which can be attributed to its affinity towards the negatively charged DNA.

3.2 Binding efficiency of nanoparticles

For the binding efficiency studies, the amount of dystrophin plasmid (18.8 kb) was kept constant at 50 ng and the amount of R-HAp Nps in the complex varied between 100 and 500 μg. Fig. 2A shows the R-HAp : plasmid complex incubated for 20 minutes at room temperature and run on agarose gel. Complete retention of the plasmid was observed from 400 μg by weight of the R-HAp Nps. Between 100 and 300 μg of R-Hap, the retention was incomplete. Hence, further experiments were carried out by maintaining the ratio of 50 ng of plasmid to 400 μg of R-HAp. Initially, we studied the binding efficiency of the dystrophin plasmid with our previously published octa arginine modified HAp nanoparticles (R8 HAp), which had demonstrated efficient binding to siRNA. However, it was observed that for large sized plasmids such as the dystrophin plasmid, the binding efficiency of R8 HAp was not very high and even at high concentrations between 600 and 800 μg by weight, it did not show retention in the agarose gel (Fig. 2B). Hence, all further studies were restricted to R-Hap Nps.

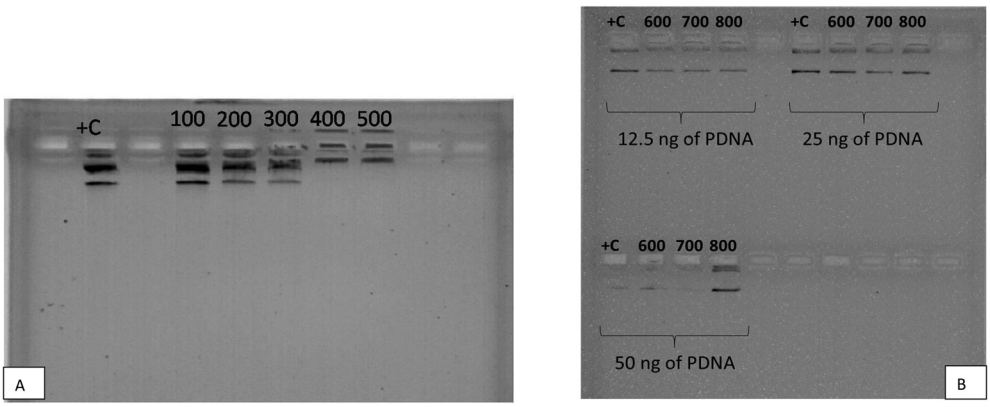

Fig. 2 Binding efficiency of (A) 100–500 μg of R-HAp with dystrophin plasmid (50 ng) and (B) 600–800 μg of R8 HAp with dystrophin plasmid (12.5, 25 and 50 ng). Unbound plasmid loaded on gel served as a positive control (+C).

3.3 MTT assay to confirm the biocompatibility of R-HAp

Biocompatibility studies of R-HAp evaluated in C2C12 cells showed no significant cytotoxicity as compared to the untreated control cells in the range of 50–500 μg ml^{-1} and cells incubated for 24 to 48 hours (Fig. 3). The one-way ANOVA test carried out to ascertain the significant change after treatment with R-HAp nanoparticles showed that there was no significant change between the control and transfected cells at 24 hours (p = 0.866847, α = 0.05) and 48 hours (p = 0.895082637 α = 0.05). This demonstrates the biocompatibility of R-HAp and corroborates our earlier study on R-HAp (0.1% by weight) on *C. albicans* cells and R8 HAp on mouse embryonic stem cells.[11,18]

3.4 Evaluation of transfection efficiency of R-HAp by gene expression analysis

To evaluate the transfection potential of the plasmid : R-HAp conjugate (50 ng of dystrophin plasmid to 400 μg of R-HAp), the undifferentiated (myoblasts) and differentiated (myotubes) mouse skeletal muscle cells (C2C12) were used as the model. The transfection efficiency was studied by incubating with this complex and the expression of the reporter gene mCherry was visualized 48 h post incubation. As shown in Fig. 4, the expression of mCherry was evident by the bright red fluorescence observed in the cytoplasmic area of the undifferentiated (Fig. 4A–C) and the differentiated (Fig. 4D and E) cells after 48 hours of delivery of the conjugate. The percentage of transfection efficiency, calculated as the ratio of the number of transfected cells to the total number of cells present, was found to be high and almost all the cells expressed red fluorescence in both myoblasts and myotubes for R-Hap-mediated transfection.

As compared to this, a much weaker fluorescence intensity was observed upon using the commercially available transfection reagent Lipofectamine 3000 (Fig. 4B and C). Moreover, it is important to note that as per the manufacturer's protocol, a 20-fold higher amount of the plasmid DNA (1 μg, as opposed to 50 ng) was used for transfection analysis with Lipofectamine.

The one-way ANOVA test with a p value of 5.34×10^{-10} between the groups showed that there was a significant difference between the CTCF values of the control cells, Lipofectamine-transfected cells and R-Hap-transfected cells.

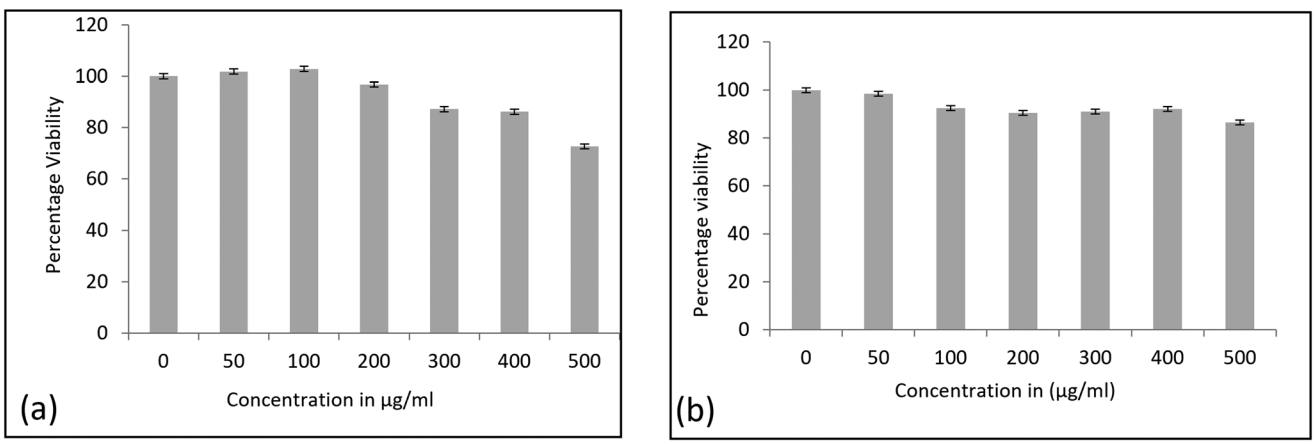

Fig. 3 MTT assay of R-HAp nanoparticles after (A) 24 hours (p = 0.866847) and (B) 48 hours (p = 0.895082637) of incubation statistically analyzed by one way ANOVA (mean ± SD, n = 3), α = 0.05.

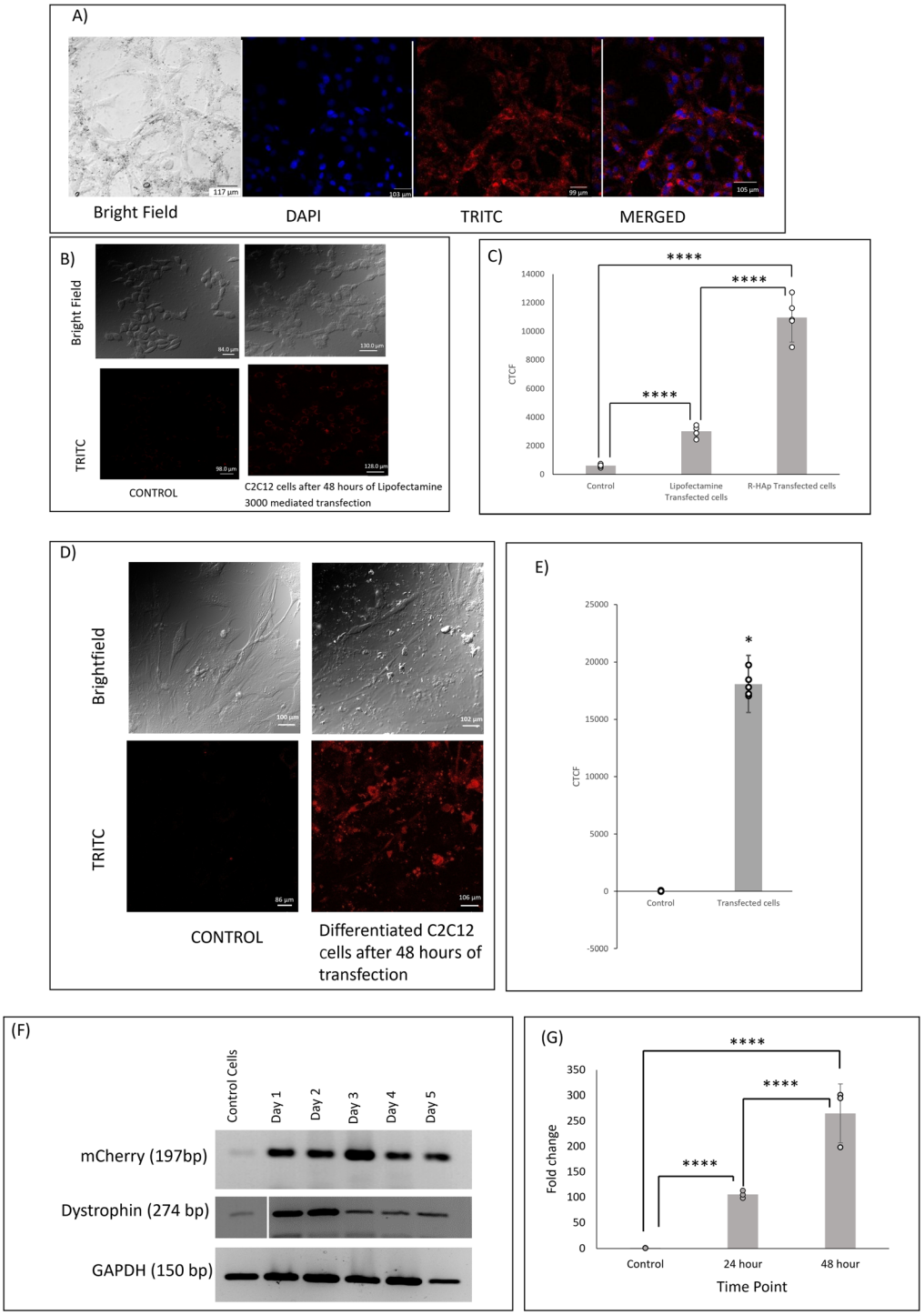

Fig. 4 Confocal study of dystrophin plasmid delivery in undifferentiated C2C12 myoblasts. (A) C2C12 cells transfected using 400 μg of R-HAp conjugated with 50 ng of plasmid. The expression of the reporter gene mCherry, present in the plasmid backbone, was observed 48 hours post delivery. (B) Control cells and C2C12 cells transfected with 1 μg of plasmid using Lipofectamine 3000. (C) Graphical representation of CTCF (corrected total cell fluorescence) for control cells, R-HAp transfected cells and Lipofectamine 3000 transfected cells (one way ANOVA test with Tukey's test as a post hoc test, n = 5, **** indicates highly significant difference amongst groups). (D) Confocal study of dystrophin plasmid delivery in differentiated C2C12 myotubes by 400 μg of R-HAp conjugated with 50 ng of plasmid, 48 hours post transfection. (E) Graphical representation of CTCF values of the controls and the transfected cells along with one sample T-test results (mean ± standard deviation, n = 5, α = 0.05), *P < 0.05. (F) Expression of mCherry gene, dystrophin and GAPDH by RT-PCR analysis of the transfected mouse myotubes. [Control cells: untransfected cells; day 1–day 5: RNA extracted from cells post transfection from day 1 to day 5.] (G) q-PCR analysis of mCherry gene expression in R-HAp mediated transfected C2C12 cells, 24 and 48 h post transfection. Fold change was calculated with respect to the untransfected control cells and the values were normalized against 18S as an internal control. (Bar graphs (mean ± standard deviation, n = 3) represent the one way ANOVA single factor test along with Tukey's test as a post hoc test, n = 3, **** indicates highly significant difference amongst groups).

Furthermore, Tukey's HSD test revealed that the mean CTCF values were significantly different between all three groups as shown in Fig. 4C ($p < 0.001$). A one sample *T*-test showed a statistically significant difference between the CTCF values of transfected myotubes and untransfected myotubes with $p < 0.05$.

These results highlighted the efficacy of R-HAp for carrying a large plasmid of 18.8 kb to both the differentiated and undifferentiated mouse skeletal muscle cells with better efficiency than the commercially available transfection reagent.

To further confirm the above results, mRNA expression analysis by RT-PCR was performed for the mCherry and dystrophin genes in the transfected mouse myotubes and the expression compared with that in the untransfected control cells. The mCherry reporter gene and dystrophin expression at the mRNA level were observed from day 1 to day 5 post-delivery (Fig. 4F).

Analysis of mCherry gene expression was also performed using qPCR (Fig. 4G). Compared to the untransfected control cells, approximately 166 ± 37 and 277 ± 96 fold changes in the expression were observed 24 and 48 hours post transfection, respectively. The values were normalized using 18S as a housekeeping gene. The one-way ANOVA test revealed that the fold change between the groups was significant with a *p*-value of 0.000211. Tukey's test results showed that fold change amongst control and transfected cells (24 hours and 48 hours) was significant.

These results reemphasize the ability of R-HAp to successfully transfect the dystrophin plasmid into skeletal muscle cells with a very high efficiency using only 50 ng of plasmid.

3.5 Confocal microscopy to confirm the transfection in normal human skeletal muscle cells

The efficiency of the R-HAp mediated transfection was also tested in normal human skeletal muscle cells and expression of the mCherry gene was evident from the confocal microscopy images (Fig. 5). The R-HAp transfection efficiency in these cells was found to be 75.6 ± 22%, indicating that primary cells exhibit lower transfection efficiency as compared to C2C12 cells as reported earlier.[19]

3.6 Analysis of dystrophin gene expression in the skeletal muscle cells derived from the skin fibroblasts of a DMD patient

As per the main objective of this study, we next tested the efficacy of R-HAp Nps to deliver the dystrophin gene in patient skeletal muscle cells. These cells were derived from the skin fibroblasts of a patient, whose dystrophin gene is non-functional and does not express due to a mutation in exon 44. To check for the cytotoxicity of R-HAp Nps with skin fibroblast cells, an MTT assay was performed. As seen in Fig. 6, even after 24 hours of constant exposure to the Nps, there was no significant cell death up to a concentration of 500 μg ml^{-1}. The results from the one-way ANOVA test show that the *p* value was 0.117067 between the groups showing that statistically there was no significant change between the cell viability of the control cells and that of the treated cells. It is important to note that for the gene delivery study, the cells were exposed to the nano-complex only for

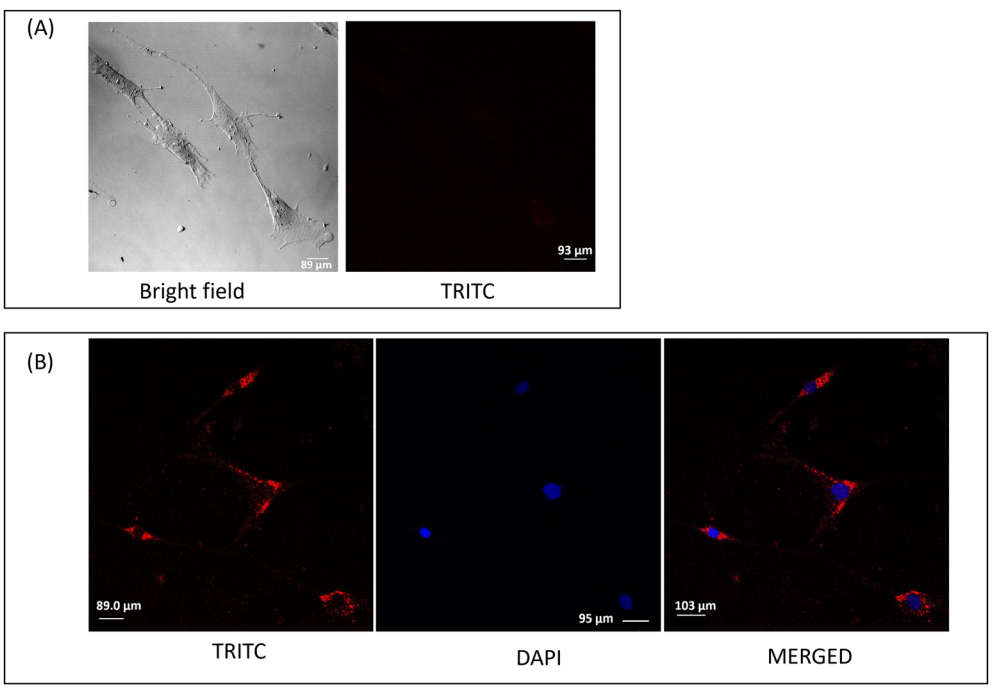

Fig. 5 (A) Un-transfected human skeletal muscle cells. (B) R-HAp mediated transfection of an 18.8 kb plasmid in normal human skeletal muscle cells. (Images are obtained 48 hours post transfection.)

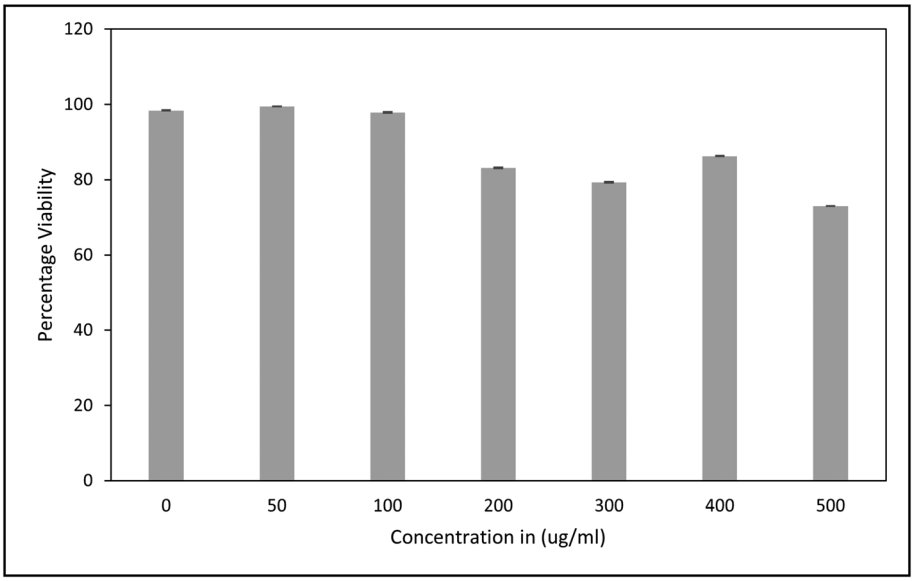

Fig. 6 MTT assay after 24 hours of incubation of patient myotube cells with R-HAp confirming no cytotoxicity. The data were statistically analyzed using one way ANOVA (mean ± SD, $n = 3$), $p = 0.117067$, $\alpha = 0.05$.

6 hours at a concentration of 400 μg ml^{-1}, subsequent to which a wash and a media change were given to the cells.

Expression of the reporter gene mCherry was evident in the fibroblast derived skeletal muscle cells in a time dependent manner, 24 and 48 hours post delivery of the nano-complex (Fig. 7A, and B respectively and quantification is shown in Fig. 7C). A one sample *T*-test showed a statistically significant difference between the CTCF values of transfected cells and those of untransfected cells with $p < 0.05$.

To test the expression of the dystrophin gene in these cells, RT-PCR analysis was performed with the primers designed against exons 43 to 45. Total RNA was harvested from day 1 to day 5 post delivery of the complex. As shown in Fig. 8, transfected patient cells showed an overexpression of the dystrophin gene over the span of 5 days as compared to the expression of the endogenous gene in the un-transfected cells. Analysis of an internal control, GAPDH, showed a similar expression pattern in both the groups (Fig. 8).

Western blot analysis (Fig. 9) further confirmed the overexpression of dystrophin protein in the DMD patient cells 7 days post transfection compared to the un-transfected control.

These results clearly demonstrate that the R-HAp nanocarrier was successful in delivery and expression of the dystrophin gene at both the mRNA and protein levels in the patient derived skeletal muscle cells. This method of delivery shows no sign of toxicity to these cells and thus the potential of R-HAp as a promising gene delivery agent in DMD patients should be further explored.

4 Discussion

Duchenne muscular dystrophy is an X chromosome linked disease. Treatment methods vary from physiotherapy and drugs to gene therapy. The gene therapy method involves delivery of either full or partial functional segments (micro or mini) of dystrophin gene to the cells. The delivery of mini or micro dystrophin segments attenuates some of the symptoms but does not cure the disease. The delivery of a full-length dystrophin gene which is 11.5 kb long (coding sequence) is expected to eliminate all the symptoms. Conventionally used AAV vectors are not suitable for dystrophin gene delivery due to their limited cargo carrying capacity of 4.2 kb, which has led to a search for alternative non-viral vectors to deliver the full length gene.

Another approach for delivery of the full-length dystrophin gene is using a dual AAV vector-based hybrid system. This method however, has not shown good potential in pre-clinical trials due to triggering of the host immune response and low expression of the dystrophin gene in skeletal muscle cells post delivery.[20] In addition, the production cost for AAV vectors is very high owing to the need for specialized viral production facilities, purification techniques and stringent quality control measures.[21] These drawbacks limit the usage of viral vectors in DMD therapeutics.

In this study, we show that inorganic calcium based nanocarriers, R-HAp Nps, exhibit the potential to deliver the 18.8 kb DMD plasmid to normal mouse and human skeletal muscle cells, as well as DMD patient cells. This study is an excellent example of non-viral delivery of large genes in normal as well as difficult to transfect primary cells.[19]

R-HAp Nps were synthesized and characterized as per the previous reports from our lab.[16] The characterization studies indicated that arginine modification was successful with the nanoparticles showing a pure phase of R-HAp. The present study has shown that these nanoparticles are able to deliver large nucleic acid molecules in addition to siRNAs as reported

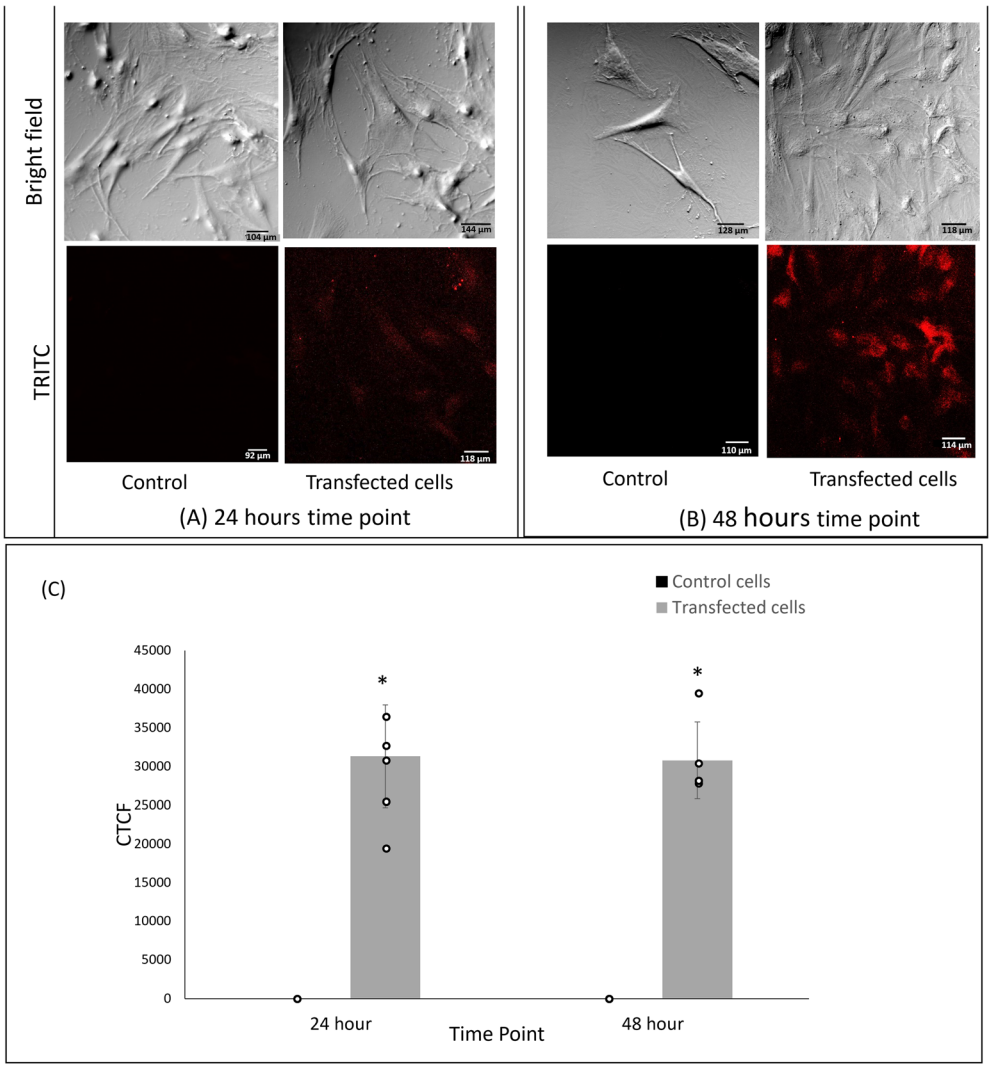

Fig. 7 R-HAp mediated transfection of the 18.8 kb dystrophin plasmid in DMD patient cells. Confocal images obtained after (A) 24 hours and (B) 48 hours post transfection. (C) Graphical representation of CTCF data displaying one sample *T*-test results (mean ± standard deviation, $n = 5$), $*p < 0.05$.

earlier.[11] As per our literature survey, we have not found any report on delivering the full length dystrophin plasmid using nanoparticles; thus, this is the first study to report the transfection of full length dystrophin using R-HAp Nps.

Dendrimer based nanoparticles have been used to deliver micro-dystrophin plasmids *in vitro* as well as *in vivo*; however, a large amount of plasmid was required for transfection in different cell types (4.5 μg).[22] In contrast, the transfection experiments using R-HAp Nps use a very low amount of plasmid (50 ng) for the expression of the dystrophin gene. It is important to note that this amount is 20-fold lower as compared to the commercial transfection agent Lipofectamine 3000. A similar amount of DMD-plasmid requirement was also reported using Xfect transfection reagent in HEK-293 cells.[12] This indicates that while R-HAp mediated transfection uses much less plasmid in comparison with other delivery agents, it exhibits internalization and gene expression with very high efficiency.

For DMD therapeutics, nanoparticle based delivery of antisense oligonucleotides for the exon skipping mechanism targeting the splicing pattern of the dystrophin gene at the pre-mRNA level is also explored. These include lipid and polymer based nanoparticles,[23] polymersomes,[24] cell penetrating peptides,[25,26] polyethyleneimine *etc*. However, most of these methods face the challenges of slow biodegradation, aggregate formation, toxicity due to structure and molecular weight and associated adverse effects during treatment.[27,28] In comparison, R-HAp Nps are biodegradable and biocompatible as the chemical composition of R-HAp Nps is similar to the inorganic content in human bones. This gives R-HAp an edge over other nanoparticles in being safe to be used as a gene delivery agent. In addition, since a very small amount of plasmid is used, this

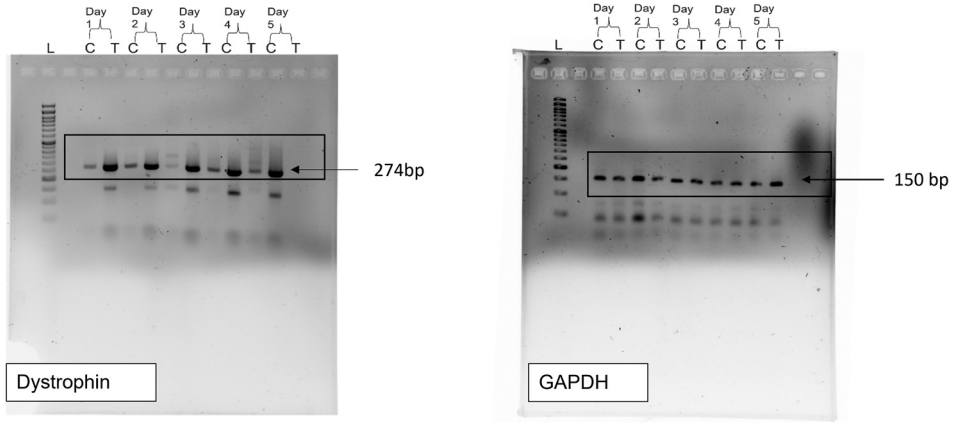

Fig. 8 RT-PCR analysis of the dystrophin and GAPDH gene expression from patient myotubes. RNA was harvested from the R-HAp mediated dystrophin plasmid transfected (T) and un-transfected (C) patient myotubes, 1–5 days post delivery.

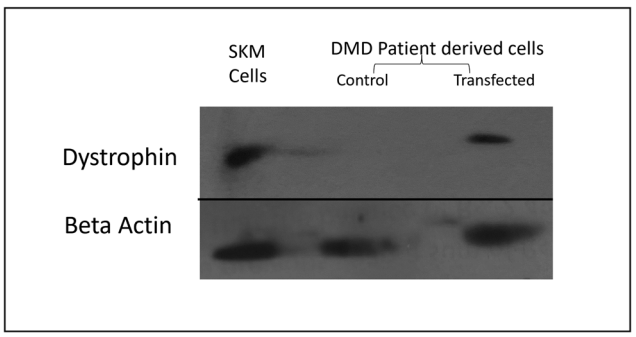

Fig. 9 Western blot analysis of dystrophin and β-actin protein. Protein was extracted from untransfected DMD patient cells and transfected DMD patient cells. Normal human skeletal muscle cells (SKM) served as the positive control for dystrophin protein expression.

platform will be cost effective for practical purposes. A rough estimate of the cost to synthesize 10 ml of R-HAp sol is <1$. Another factor that gives an added advantage with R-HAp Nps is their ability to escape endosomal degradation by the proton sponge effect. These nanoparticles owing to their pH buffering capacity trigger osmotic rupture which leads to endosomal degradation. The internalization of these nanoparticles in the cells was attributed to the endocytosis mechanism wherein it was shown they are mainly taken up by clathrin mediated endocytosis and micropinocytosis.[29]

The transfection efficiency of the nano-conjugate was also tested in the DMD-patient skeletal muscle cells derived from their skin fibroblasts. The nano-vehicle showed excellent biocompatibility and delivery efficiency of the full-length dystrophin gene in these cells, at both the mRNA and protein levels at least up to five and seven days respectively, post delivery of the nano-conjugate.

Taken together, our results indicate that R-HAp Nps have excellent potential for gene delivery-based therapeutics, especially where the large plasmid size is a limiting factor and the use of viral vectors becomes challenging. Moreover, a minimal amount of plasmid is required for successful gene delivery, while exhibiting sustained expression, with negligible cytotoxicity. This could be an attractive cost-effective alternative to the 'million dollar therapy' using AAV vectors.

5 Conclusion

In conclusion, our findings indicate R-HAp nanoparticles are excellent candidates for delivering a large gene like dystrophin plasmid (18.8 kb). These nanoparticles were able to transfect the mouse and human skeletal muscle cells with a much smaller amount of plasmid as compared to the commercial transfection agent. Transfection into patient derived myotubes showed robust over-expression of the dystrophin gene and protein. These results indicate that R-HAp NPs exhibit excellent potential as gene delivery agents for DMD as well as for other genetic diseases where the delivery of large genes is expected.

Author contributions

All authors contributed to the study's conceptualization and design. Pooja Kotharkar performed the experiments, data collection and analysis and wrote the first draft of the manuscript. Prof. Sutapa Roy Ramanan helped with the synthesis and characterization of hydroxyapatite nanoparticles. Dr Arun Shastry helped with providing facilities for DMD patient cell related experiments. Corresponding authors, Prof. Meenal Kowshik and Prof. Indrani Talukdar helped with experimental designs and reviewed the manuscript.

Ethical approval

Ethical clearance for conducting *in vitro* experiments using skin fibroblast cells from DMD positive patients was provided by DART, Bangalore.

Data availability

The data supporting this article have been included as part of the ESI.†

Conflicts of interest

The authors declare no competing interest.

Acknowledgements

This research work was financially supported by the ICMR grant number 33/21/2023/RD/BMS and DBT Builder-BITS Pilani K K Birla Goa Campus Interdisciplinary Life Science Programme for Advanced Research and Education (Level III) BT/INF/22/SP2543/2021. The study also partially benefitted from the professional development fund granted to Meenal Kowshik and Indrani Talukdar by BITS Pilani, Goa. Pooja Kotharkar was also supported by the Institute Fellowship provided by BITS Pilani, K K Birla Goa Campus. The authors are thankful to the Sophisticated Analysis Instrumentation Facility, Indian Institute of Technology, Bombay, for their help with HR-TEM studies. The authors also acknowledge the Central Sophisticated Instrumentation Facility (CSIF), BITS Pilani K.K. Birla Goa Campus for help with CLSM studies.

References

1 J. C. van Deutekom and G. J. van Ommen, Advances in Duchenne muscular dystrophy gene therapy, *Nat. Rev. Genet.*, 2003, **4**(10), 774–783.
2 R. J. Fairclough, M. J. Wood and K. E. Davies, Therapy for Duchenne muscular dystrophy: Renewed optimism from genetic approaches, *Nat. Rev. Genet.*, 2013, **14**(6), 373–378.
3 C. L. Bladen, D. Salgado, S. Monges, M. E. Foncuberta, K. Kekou, K. Kosma, *et al.*, The TREAT-NMD DMD Global Database: Analysis of more than 7,000 Duchenne muscular dystrophy mutations, *Hum. Mutat.*, 2015, **36**(4), 395–402.
4 Y. L. Min, R. Bassel-Duby and E. N. Olson, CRISPR correction of duchenne muscular dystrophy, *Annu. Rev. Med.*, 2019, **70**, 239–255.
5 A. C. Koumbourlis, Scoliosis and the respiratory system, *Paediatr. Respir. Rev.*, 2006, **7**(2), 152–160.
6 Z. Wu, H. Yang and P. Colosi, Effect of genome size on AAV vector packaging, *Mol. Ther.*, 2010, **18**(1), 80–86.
7 J.-Y. Dong, P.-D. Fan and R. A. Frizzell, Quantitative analysis of the packaging capacity of recombinant adeno-associated virus, *Hum. Gene Ther.*, 1996, **7**(17), 2101–2112.
8 D. Duan, Systemic AAV micro-dystrophin gene therapy for Duchenne muscular dystrophy, *Mol. Ther.*, 2018, **26**(10), 2337–2356.
9 D. Duan, Micro-dystrophin gene therapy goes systemic in Duchenne muscular dystrophy patients, *Hum. Gene Ther.*, 2018, **29**(7), 733–736.
10 K. A. Danilov, S. G. Vassilieva, A. V. Polikarpova, A. V. Starikova, A. A. Shmidt, I. I. Galkin, *et al.*, In vitro assay for the efficacy assessment of AAV vectors expressing microdystrophin, *Exp. Cell Res.*, 2020, **392**(2), 112033.
11 P. Zantye, S. Shende, S. R. Ramanan, I. Talukdar and M. Kowshik, Design of a biocompatible hydroxyapatite-based nanovehicle for efficient delivery of small interference ribonucleic acid into mouse embryonic stem cells, *Mol. Pharm.*, 2021, **18**(3), 796–806.
12 A. P. Farruggio, M. S. Bhakta, H. du Bois, J. Ma and M. P. Calos, Genomic integration of the full–length dystrophin coding sequence in Duchenne muscular dystrophy induced pluripotent stem cells, *Biotechnol. J.*, 2017, **12**(4), 1600477.
13 T. Grimm, W. Kress, G. Meng and C. R. Müller, Risk assessment and genetic counseling in families with Duchenne muscular dystrophy, *Acta Myol.*, 2012, **31**(3), 179–183.
14 L. Lattanzi, G. Salvatori, M. Coletta, C. Sonnino, M. C. De Angelis, L. Gioglio, *et al.*, High efficiency myogenic conversion of human fibroblasts by adenoviral vector-mediated MyoD gene transfer. An alternative strategy for ex vivo gene therapy of primary myopathies, *J. Clin. Invest.*, 1998, **101**(10), 2119–2128.
15 K. P. Tank, K. S. Chudasama, V. S. Thaker and M. J. Joshi, Cobalt-doped nanohydroxyapatite: Synthesis, characterization, antimicrobial and hemolytic studies, *J. Nanopart. Res.*, 2013, **15**, 1–11.
16 K. Deshmukh, M. M. Shaik, S. R. Ramanan and M. Kowshik, Self-activated fluorescent hydroxyapatite nanoparticles: A promising agent for bioimaging and biolabeling, *ACS Biomater. Sci. Eng.*, 2016, **2**(8), 1257–1264.
17 R. Gonzalez-McQuire, J.-Y. Chane-Ching, E. Vignaud, A. Lebugle and S. Mann, Synthesis and characterization of amino acid-functionalized hydroxyapatite nanorods, *J. Mater. Chem.*, 2004, **14**(14), 2277–2281.
18 K. Deshmukh, S. R. Ramanan and M. Kowshik, A novel method for genetic transformation of *C. albicans* using modified-hydroxyapatite nanoparticles as a plasmid DNA vehicle, *Nanoscale Adv.*, 2019, **1**(8), 3015–3022.
19 F. Pampinella, D. Lechardeur, E. Zanetti, I. MacLachlan, M. Benharouga, G. L. Lukacs, *et al.*, Analysis of differential lipofection efficiency in primary and established myoblasts, *Mol. Ther.*, 2002, **5**(2), 161–169.
20 Y. Zhou, C. Zhang, W. Xiao, R. W. Herzog and R. Han, Systemic delivery of full-length dystrophin in Duchenne muscular dystrophy mice, *Nat. Commun.*, 2024, **15**(1), 6141.

21 A. Srivastava, K. M. G. Mallela, N. Deorkar and G. Brophy, Manufacturing challenges and rational formulation development for AAV viral vectors, *J. Pharm. Sci.*, 2021, **110**(7), 2609–2624.
22 J. Hersh, J. M. C. Capcha, C. I. Irion, G. Lambert, M. Noguera, M. Singh, *et al.*, Peptide-functionalized dendrimer nanocarriers for targeted microdystrophin gene delivery, *Pharmaceutics*, 2021, **13**(12), 2159–2175.
23 M. S. Falzarano, C. Passarelli and A. Ferlini, Nanoparticle delivery of antisense oligonucleotides and their application in the exon skipping strategy for Duchenne muscular dystrophy, *Nucleic Acid Ther.*, 2014, **24**(1), 87–100.
24 Y. Kim, M. Tewari, J. D. Pajerowski, S. Cai, S. Sen, J. Williams, *et al.*, Polymersome delivery of siRNA and antisense oligonucleotides, *J. Controlled Release*, 2009, **134**(2), 132–140.
25 F. Shabanpoor, G. McClorey, A. F. Saleh, P. Järver, M. J. Wood and M. J. Gait, Bi-specific splice-switching PMO oligonucleotides conjugated via a single peptide active in a mouse model of Duchenne muscular dystrophy, *Nucleic Acids Res.*, 2015, **43**(1), 29–39.
26 P. Rimessi, P. Sabatelli, M. Fabris, P. Braghetta, E. Bassi, P. Spitali, *et al.*, Cationic PMMA nanoparticles bind and deliver antisense oligoribonucleotides allowing restoration of dystrophin expression in the mdx mouse, *Mol. Ther.*, 2009, **17**(5), 820–827.
27 R. Mohammapdour and H. Ghandehari, Mechanisms of immune response to inorganic nanoparticles and their degradation products, *Adv. Drug Delivery Rev.*, 2022, **180**, 114022.
28 R. Rai, S. Alwani and I. Badea, Polymeric nanoparticles in gene therapy: New avenues of design and optimization for delivery applications, *Polymers*, 2019, **11**(4), 745.
29 P. Zantye, I. Talukdar, S. R. Ramanan and M. Kowshik, Self-fluorescence property of octa-arginine functionalized hydroxyapatite nanoparticles aids in studying their intracellular fate in R1 ESCs, *Biochem. Biophys. Res. Commun.*, 2022, **627**, 21–29.